



鄂尔多斯盆地西缘及邻区石炭系羊虎沟组砂体成因机制与沉积过程

朱淑玥, 刘磊, 王峰, 侯云东, 王志伟, 张成弓, 付斯一, 陈洪德, 张靖芪

引用本文:

朱淑玥, 刘磊, 王峰, 侯云东, 王志伟, 张成弓, 付斯一, 陈洪德, 张靖芪. 鄂尔多斯盆地西缘及邻区石炭系羊虎沟组砂体成因机制与沉积过程[J]. 沉积学报, 2023, 41(4): 1153-1169.

ZHU ShuYue, LIU Lei, WANG Feng, HOU YunDong, WANG ZhiWei, ZHANG ChengGong, FU SiYi, CHEN HongDe, ZHANG JingQi. Genetic Mechanism and Depositional Processes of Sandy Sediments from the Carboniferous Yanghugou Formation Along the Western Margin of the Ordos Basin and Its Adjacent Areas[J]. *Acta Sedimentologica Sinica*, 2023, 41(4): 1153-1169.

相似文章推荐 (请使用火狐或IE浏览器查看文章)

Similar articles recommended (Please use Firefox or IE to view the article)

曲流河三角洲—辫状河三角洲控制因素及演化过程探讨

Control Factors and Evolution Progress of Depositional System Transition from Meandering River Delta to Braided River Delta: Case study of Shan2 member to He8 member, Ordos Basin

沉积学报. 2019, 37(4): 768-784 <https://doi.org/10.14027/j.issn.1000-0550.2018.154>

鄂尔多斯盆地西缘上三叠统延长组沉积相特征研究

Study on Sedimentary Facies Features of the Upper Triassic Yanchang Formation, in the Western Margin, Ordos Basin

沉积学报. 2019, 37(1): 163-176 <https://doi.org/10.14027/j.issn.1000-0550.2018.156>

沾化凹陷孤岛西部斜坡带沙三段重力流沉积特征与源—汇体系

Depositional Characteristics and Source to Sink Systems of Gravity Flow of the Third Member of Shahejie Formation in Gudao West Slope Zone of Zhanhua Sag, Bohai Bay Basin, China

沉积学报. 2018, 36(3): 542-556 <https://doi.org/10.14027/j.issn.1000-0550.2018.076>

牛庄洼陷沙三中亚段三角洲—重力流体系沉积特征与模式

Sedimentary Characteristics and Depositional Model of Delta and Gravity Flow System of the Middle Member 3 of Shahejie Formation in Niuzhuang Sag

沉积学报. 2018, 36(2): 376-389 <https://doi.org/10.14027/j.issn.1000-0550.2018.027>

渤中西环古近系东营组物源转换与沉积充填响应

The Provenance Transformation and Sedimentary Filling Response of Paleogene Dongying Formation in Western Slope of Bozhong Sag

沉积学报. 2015, 33(1): 36-48 <https://doi.org/10.14027/j.cnki.cjxb.2015.01.004>

文章编号:1000-0550(2023)04-1153-17

DOI: 10.14027/j.issn.1000-0550.2022.001

鄂尔多斯盆地西缘及邻区石炭系羊虎沟组砂体成因机制与沉积过程

朱淑玥¹, 刘磊^{1,2}, 王峰^{1,2}, 侯云东³, 王志伟¹, 张成弓^{1,2}, 付斯一^{1,2}, 陈洪德^{1,2}, 张靖芪¹

1. 成都理工大学沉积地质研究院, 成都 610059

2. 油气藏地质及开发工程国家重点实验室(成都理工大学), 成都 610059

3. 中国石油长庆油田分公司勘探开发研究院, 西安 710000

摘要 鄂尔多斯盆地西缘羊虎沟组时期为加里东运动后复活的拗拉槽, 羊虎沟组分布面积广, 厚度变化大, 发育良好的生储盖组合, 具有巨大的勘探潜力。由于该地区构造运动强烈, 沉积环境变化频繁, 致使砂体沉积成因复杂。目前对羊虎沟组砂体成因机制缺乏系统研究, 单一的沉积模式无法全面概括各类砂体的沉积特征与展布规律。通过野外剖面、岩心观察、钻井资料、物源分析等方法, 共识别出6种岩相组合类型。基于岩性、粒度、沉积构造及各时期砂体展布等特征, 对其成因机制及沉积过程进行了系统讨论。鄂尔多斯盆地西缘羊虎沟组砂体成因主要为河控三角洲、潮控三角洲、扇三角洲、障壁岛海岸、无障壁海岸和滑塌重力流6类。羊虎沟组时期整体气候潮湿, 羊三段至羊二段沉积时期海平面逐渐上升, 至羊二段达到最高之后逐渐下降。羊三段沉积时期为裂陷早期, 主要在研究区北部发育潮控三角洲和扇三角洲砂体, 中部局部可见潮汐砂脊砂体, 南部砂体整体表现为无障壁海岸沉积。羊二段沉积时期为裂陷高潮期, 地貌落差加大致使水体快速变深, 砂体主要分布于盆地边缘; 盆地中央深水部位发育点状滑塌重力流砂体, 东部靠近中央古隆起一侧的潮汐砂脊逐渐被改造为障壁沙坝, 古隆起高部位则为潮坪和潟湖沉积。羊一段沉积时期, 构造活动减弱且鄂尔多斯盆地逐渐东西连通, 物源供应充足, 地貌变缓, 发育大面积具前积特征的河控三角洲砂体。羊虎沟组砂体成因机制受构造运动、古地貌演化、物源供给、古气候、海平面变化等多因素共同影响, 但砂体展布与沉积过程主要受控于构造活动与古地理演化。该研究成果丰富了鄂尔多斯盆地油气勘探理论和裂陷盆地砂体成因机制。

关键词 岩相组合; 成因机制; 控制因素; 砂体展布; 羊虎沟组; 鄂尔多斯盆地西缘

第一作者简介 朱淑玥, 女, 1997年出生, 硕士研究生, 地质学, E-mail: zhushuyue0309@163.com

通信作者 刘磊, 男, 研究员, E-mail: 172058088@qq.com

中图分类号 P618.13 **文献标志码** A

0 引言

鄂尔多斯盆地是我国大型含油气盆地之一, 蕴藏丰富的油气资源。其西缘位于华北陆块和秦祁昆造山带两个性质迥然不同的一级大地构造单元之间近南北向的狭长地带^[1], 是我国北方东西部不同构造单元的连接地区^[2-4]。近年来, 专家学者开始关注鄂尔多斯盆地西缘及其邻区的油气勘探潜力^[5-8], 多期次的构造活动直接影响研究区的古地理格局、物源方向、砂体沉积厚度和岩性等^[9], 砂体时空展布和成

因机制的差异决定了鄂尔多斯盆地西缘羊虎沟组生储盖层的有利组合^[10]。

鄂尔多斯盆地西缘从晚石炭世早期前黑山组开始接受沉积, 晚石炭世末期羊虎沟组大致与华北克拉通的本溪组相当^[11-12]。羊虎沟组在盆地西缘分布面积较广, 厚度变化较大, 是良好的烃源岩地层^[3]。受沉积模式认识差异影响, 不同学者对砂体成因持有不同观点, 大部分学者认为鄂尔多斯盆地西缘羊虎沟组时期主要发育潮控三角洲和障壁岛海岸沉积体系, 有学者认为还发育了浅海陆棚和扇三角洲沉

收稿日期: 2021-11-01; 修回日期: 2022-01-02; 录用日期: 2022-01-21; 网络出版日期: 2022-01-21

基金项目: 国家自然科学基金项目(42102132); 中石油长庆油田资助项目(2020-62503) [Foundation: National Natural Science Foundation of China, No. 42102132; CNPC Changqing Oilfield Funded Project, No. 2020-62503]

积体系^[13-17]。受构造运动影响,该地区沉积环境变化频繁,砂体沉积类型多样。目前对羊虎沟组砂体形成和沉积过程的认识较为薄弱,单一的沉积模式无法很好地解释研究区砂体复杂的成因机制和较强的非均质性。综上所述,本文基于研究区乌达、呼鲁斯太等10余处野外露头剖面的勘察研究,以及对巴参2井、阿参1井等40余口井位的岩心观察及钻井等资料,通过系统研究鄂尔多斯盆地西缘及其邻区羊虎沟组砂体的沉积特征,阐明其成因机制,揭示其展布规律与沉积过程,并进一步明确其主要控制因素,以丰富鄂尔多斯盆地油气勘探理论,促进裂陷盆地砂体成因机制和沉积过程的研究。

1 区域地质概况

鄂尔多斯盆地西缘位于华北克拉通西部,地跨陕、甘、宁、蒙,研究区北起内蒙古乌海市,南经宁夏银川、同心、海原至环县一带,东始陕西定边、内蒙古鄂托克前旗。主体呈南北向展布,在区域大地构造位置上,鄂尔多斯盆地西缘构造带位于鄂尔多斯地块、阿拉善地块和北祁连构造带三大构造单元交汇地区,是连接中国东西部不同大地构造单元的枢纽地带(图1a)^[2,8,18]。研究区内见鄂尔多斯盆地六大构造单元中的伊盟隆起、西缘逆冲带、天环凹陷和伊陕斜坡四个构造单元,以及阿拉善地块东部的巴彦浩特盆地(图1b)。这种特殊的构造位置使其在不同地质历史时期经历了多期次拉张裂陷、挤压闭合活动^[2-4,7,19]。

石炭纪一二叠纪冈瓦那大陆不断向北运动,特提斯洋被阻,古亚洲洋封闭,泛大陆逐渐形成^[20]。在奥陶纪末期,加里东运动使华北克拉通大面积抬升,造成大面积海退^[11,21]。早石炭世,盆地西缘贺兰山拗拉槽发生横向拉张复活,形成狭窄的裂陷盆地,祁连海沿该裂陷带侵入盆地^[22-24]。晚石炭世,鄂尔多斯地区经过长期剥蚀后,又有海水侵入,缓慢沉降并接受沉积^[21,25],区内海水时进时退,以温暖湿润气候为主,为低能的闭塞海湾或湖沼潮湿环境^[14]。晚石炭世盆地中央古隆起横跨盆地南北,分割祁连海与华北海^[1],位于古隆起西部的祁连—贺兰海域形成了海陆交互相含煤沉积的羊虎沟组^[26-27],到早二叠世早期古隆起进一步沉降,形成统一陆表海^[1]。研究区北部沉积物来源于盆地西北部的阿拉善古陆和东北部的阴山古陆,南部沉积物来源于北祁连

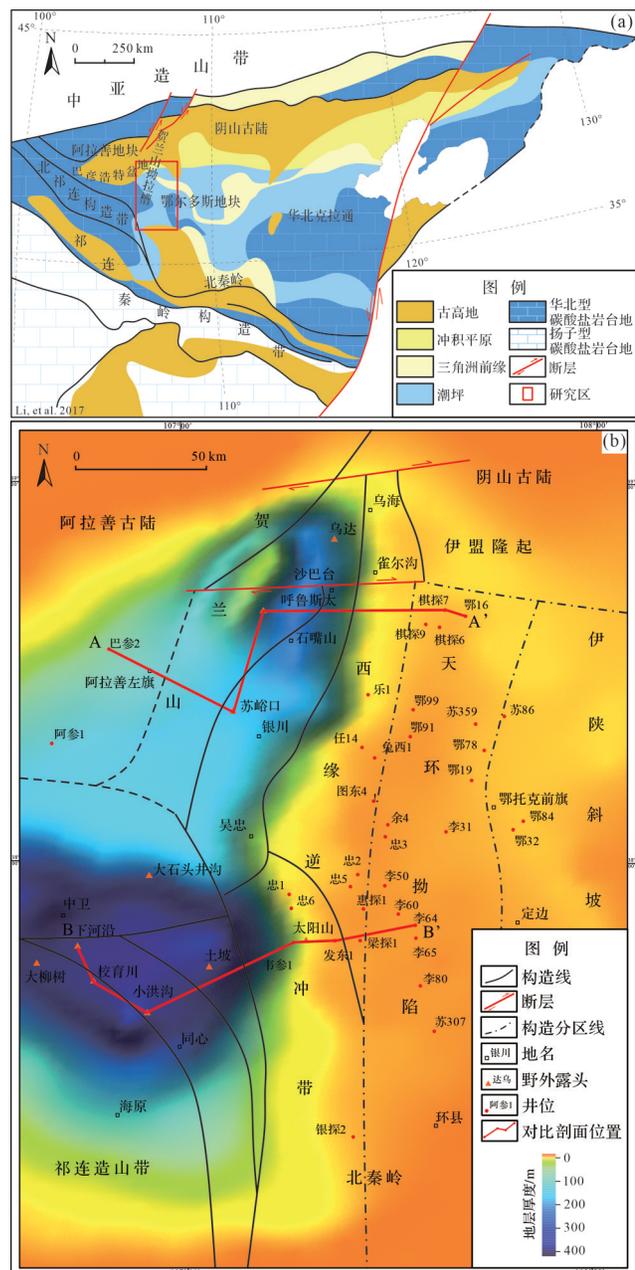


图1 鄂尔多斯盆地西缘构造位置图

(a)华北克拉通构造纲要图(据Li et al.^[18]修改);

(b)鄂尔多斯盆地西缘羊虎沟组地层厚度及构造区划图

Fig.1 Tectonic map of the western margin of the Ordos Basin

和北秦岭造山带^[4,28-34]。

2 羊虎沟组地层特征

鄂尔多斯盆地西缘祁连海域石炭纪一二叠纪沉积地层自下而上划分为石炭系前黑山组、臭牛沟组、靖远组、羊虎沟组,其上为二叠系太原组、山西组、石盒子组和石千峰组。石炭系前黑山组、臭牛沟组地

层以粗碎屑岩及大套厚层生物灰岩为特征,靖远组以黑色泥页岩广泛发育为特征。太原组主要为灰白色细砂岩、灰—灰黑色泥岩、碳质泥岩、煤层。下二叠统太原组、山西组发育海陆交互碎屑岩沉积,上二叠统石盒子组、石千峰组发育河流相碎屑岩沉积(图2a)^[4,35]。

鄂尔多斯盆地西缘羊虎沟组为上古生界石炭系地层,可划分为羊三段、羊二段和羊一段。羊虎沟组岩性主要为灰白色(含砾)石英砂岩,与灰黑色粉砂岩和黑色泥岩呈韵律性互层,夹少量灰岩和薄煤层^[8,11,18]。羊三段以中细砂岩为主,夹薄层煤、灰黑色泥岩和灰色泥质粉砂岩,地层厚度为300~450 m;羊二段为灰黑色泥岩与灰色细—粗砂岩呈不等厚互层,夹薄层煤、灰色泥质粉砂岩和深灰色粉砂质泥岩,见植物化石,地层厚度为400~500 m;羊一段以灰黑色泥岩为主,与灰色中—细砂岩、灰色泥质粉砂岩和深灰色粉砂质泥岩组成韵律层,夹薄层煤,见植物和介壳化石,地层厚度为100~150 m。羊虎沟组与上覆太原组和下伏靖远组均呈整合接触,与奥陶系或更老地层呈不整合接触(图2b)^[3,8,26,36]。

羊虎沟组分布于甘肃靖远、景泰、武威一带,是加里东运动后石炭纪祁连海逐渐向东推进到鄂尔多斯盆地西缘的沉积产物^[8],在祁连海域海侵时范围扩大到最大,并越过中央古隆起与华北海域连通。研究区东部鄂托克旗一定边一带因发育在中央古隆起之上,因此沉积厚度较薄,环县以西越过中央古隆

起,沉积厚度迅速加大,总体呈西厚东薄的特征^[1,4,8]。

3 岩相组合及砂体成因机制

3.1 岩相组合特征

岩相是一定沉积环境中形成的岩石或岩石组合,不同岩相类型组合反映不同微相的沉积过程^[37-38],是划分沉积微相、识别砂体成因的重要依据^[39]。鄂尔多斯盆地西缘羊虎沟组中共识别出6种岩相组合。

3.1.1 岩相组合A(Gt-Sp-Sw-Sh)

A1(Gt-Sp-Sh):大型槽状、板状交错层理和平行层理灰白色含砾砂岩—砂岩—粉砂岩。砾石粒径2~5 mm,分选中等,磨圆度次圆—圆状,具向上变细的正粒序特征,粒度分布概率曲线以“滚动、跳跃加悬浮”的三段式为主。砂体呈透镜状,侧向迁移叠置,长3~8 m,厚0.2~1 m。见底冲刷,对下伏地层侵蚀强烈,最大侵蚀深度约30 cm,规模较大,长7~8 m。冲刷面之上砂体底部可见次圆—圆状砾石,分选中等—差,粒径5~20 mm,具定向性,冲刷面之下见碳质泥岩及煤层,煤层平均厚度20 cm,层面平直,连续性好,夹于粉砂质、碳质泥岩之间延伸5~6 m。

A2(Sw-Sh):楔状交错层理和水平层理浅灰色中细砂岩—粉砂岩。结构及成分成熟度较高,为向上变粗的逆粒序特征,粒度分布概率曲线以“一跳一悬加过渡”的三段式为主。

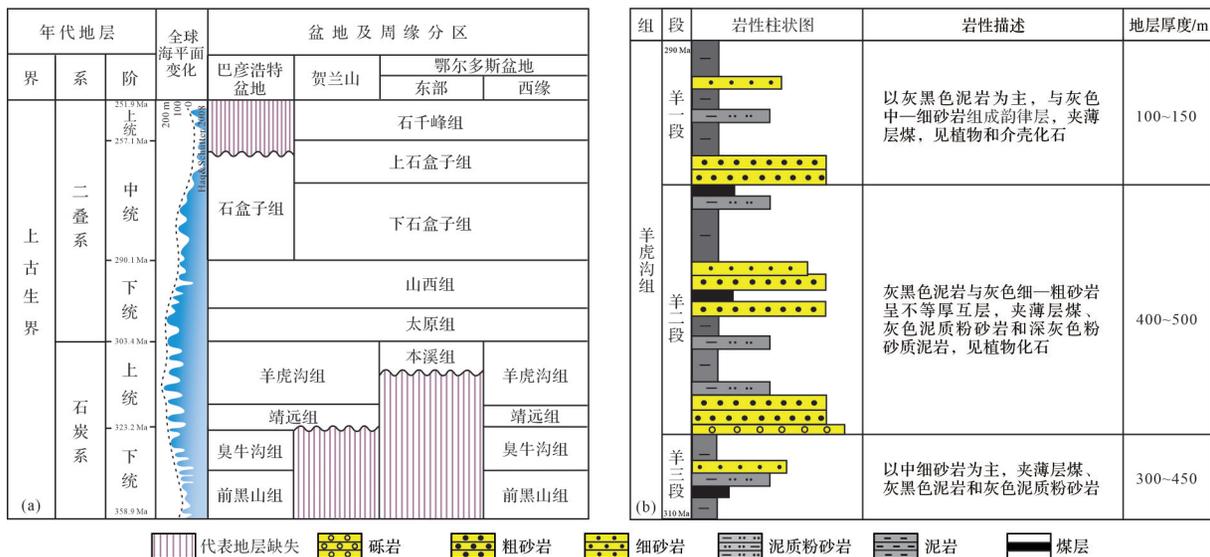


图2 研究区及周缘地层、岩性特征

(a)鄂尔多斯盆地西缘及周缘石炭纪—二叠纪地层分布图(据 Haq et al.^[35]修改);(b)鄂尔多斯盆地西缘羊虎沟组岩性综合柱状图

Fig.2 Strata and lithological characteristics of the study area and its periphery

3.1.2 岩相组合 B(Gm-St-Sf-Sp-Fc-Sw-M)

B1(Gm-St-Sf-M):小型槽状、羽状交错层理灰白色含砾中粗砂岩—细砂岩。砾石粒径2~5 mm,整体粒度较粗,颗粒支撑,发育与A1类似的粒序及粒度特征,粒度分布概率曲线以跳跃搬运为主。砂体顶平底凹,发育小规模底冲刷,冲刷面底部可见次棱角状砾石,分选差,粒径2~50 mm,砂岩内见介壳化石。冲刷面之下碳质泥岩内夹煤线,层面呈波状,连续性差。

B2(Sf-Sp-Fc):羽状、板状交错层理和脉状层理浅灰色粉—细砂岩,夹灰黑色泥质条带。整体砂质含量高,具向上变细的正粒序特征,泥岩中见虫孔。

B3(Sf-Sp-Sw):羽状、楔状和板状交错层理浅灰色中粗砂岩。结构及成分成熟度高,具向上变细的正粒序特征,粒度分布概率曲线以滚动搬运为主。见前积层理,沿水平方向层厚较稳定,单层系厚度20~30 cm,层系向前推覆叠置,相邻层系砂体间发育泥质披盖层。

3.1.3 岩相组合 C(Gt-Sp-Sh-M)

C1(Gt-Sp-Sh):中、小型槽状、板状交错层理和平行层理浅灰色含砾粗砂岩。砾石以石英为主并具有定向性,砾石粒径2~10 mm,颗粒支撑,基质含量小于15%,结构及成分成熟度较低,具向上变粗的逆粒序特征,粒度分布概率曲线以滚动搬运和跳跃搬运为主。

C2(Sh-M):平行层理灰黑色细砂岩—泥质粉砂岩—泥岩。浅灰色粉砂岩中见撕裂状泥砾,形状不规则,见植物碎片。

3.1.4 岩相组合 D(Fr-Sh-Sf-Sp-Fc-M-Lm-C)

D1(Fr-Sh):灰白色中粗石英砂岩—中细砂岩,水平层理和小型砂纹交错层理灰白色粉砂岩。结构及成分成熟度较高,具向上变粗的逆粒序特征,粒度概率曲线以跳跃搬运为主。砂体底平顶凸,砂岩层面见波痕。

D2(Sf-Sp-Fc-Fr):大一中型羽状、板状交错层理及脉状层理灰黑色中细砂岩—粉砂岩,灰黑色薄层泥与粉砂岩互层。砂泥接触面弯曲呈波状,具向上变细的正粒序特征,粒度概率曲线以跳跃总体和悬移总体为主。见灰白色前积砂质层夹灰黑色黏土质泥层的双黏土层,见植物碎片。

D3(M-Lm-C):水平层理黑—灰黑色泥岩,夹薄层粉砂岩。泥岩中见黄铁矿,植物叶片化石保存较

为完整,泥岩和粉砂岩中见大量煤层,部分煤层厚度可达1 m。

3.1.5 岩相组合 E(Gt-Gp-Sp-Sl)

冲洗交错层理和低角度交错层理砾岩—含砾砂岩—粉砂岩。砾石主要为石英,砾石粒径2~3 mm,颗粒分选好,磨圆度次圆—圆状,具有极高的成分和结构成熟度。单层厚度大,为2~4 m,具向上变粗的逆粒序特征。

3.1.6 岩相组合 F(Gm-Fc-M)

以含泥砾浅灰色粉细砂岩—黑色泥岩为主。整体具向上变细的正粒序特征。砂砾岩内夹泥质撕裂屑及泥砾,具定向性,砾石磨圆度较中等—好,但分选差(5~20 mm)。砂体滑塌卷入泥岩中,横向规模超过3 m,发育同沉积小断层及大量变形构造,揉皱变形沉积构造的轴向方向大体一致。

3.2 砂体成因机制分析

鄂尔多斯盆地西缘羊虎沟组相带发育复杂,根据不同类型的岩相组合、沉积构造及粒度分析等特征,认为6种岩相组合对应以下6类成因机制。

3.2.1 河控三角洲成因砂体

河控三角洲沉积特征主要表现为河道牵引流成因的单向层理特征^[15],主要对应于岩相组合A。砂体粒度较粗且为正粒序,砂砾岩底部见大规模底冲刷(图3d),反映强烈的侵蚀—充填过程,底部砾石分选磨圆较好,叠瓦状排列具定向性,指示单向水流方向。透镜状砂体侧向迁移叠置(图3b),见槽状、板状交错层理及平行层理等单向水流构造(图3a,c),对应河控三角洲水下分流河道侧向摆动沉积砂体特征。砂质较纯且为逆粒序,苏峪口粒度概率曲线表现为三段式(图3f),主要反映中等强度震荡水流沉积环境;可见楔状交错层理,对应河控三角洲远砂坝—河口坝砂体特征。

3.2.2 潮控三角洲成因砂体

由于受潮汐作用强烈影响,潮控三角洲砂体总体呈现出受韵律性双向水流影响的沉积构造,主要对应于岩相组合B。垂向层序下部主要为具有双向交错层理和生物碎屑的潮汐砂脊沉积,向上变为粒度较细的潮坪沉积,夹有交错层理的潮道砂体沉积^[40]。顶平底凹状砂体夹于砂泥互层的潮汐层理中(图4f)^[41],发育典型的羽状、小型槽状交错层理(图4c,d)。小型冲刷面凹凸不平,砾石分选磨圆中等,表明较强烈冲刷作用,反映潮汐作用环境,对应潮道

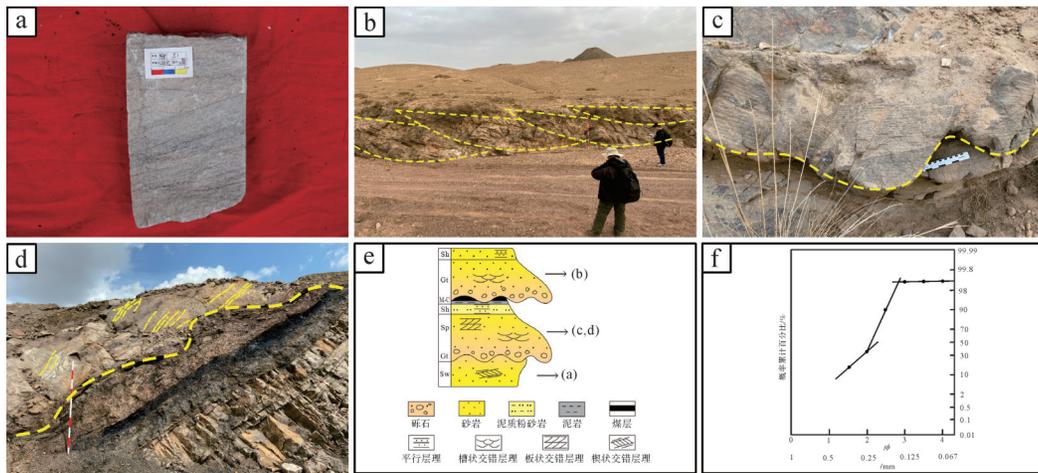


图3 鄂尔多斯盆地西缘羊虎沟组岩相组合 A 沉积特征

(a)浅灰色细砂岩,板状交错层理,羊一段,阿参1井,3 259.95 m;(b)羊虎沟组侧向迁移河道,土坡;(c)羊虎沟组水下分流河道冲刷面,土坡;(d)羊一段水下分流河道冲刷面,乌达;(e)岩相组合 A 综合柱状剖面示意图;(f)羊虎沟组水下分流河道砂岩粒度分布概率曲线图,苏峪口剖面

Fig.3 Sedimentary characteristics of lithofacies association A from the Yanghugou Formation, western Ordos Basin

砂体沉积特征^[15]。砂质含量高,夹少量泥岩层,发育的脉状层理反映供砂充分且水动力较弱的潮汐环境(图4g),对应砂坪沉积特征。不连续的透镜状砂体延伸较长且为前积状,具正粒序结构,层间夹泥质披盖层(图4b),反映砂质供给充足且水动力较强的潮汐作用环境,对应潮控三角洲前方远端潮汐砂脊特征。

3.2.3 扇三角洲成因砂体

扇三角洲是由冲积扇作为物源,在活动的扇体与稳定水体交界地带沉积的沿岸近源扇状沉积体系^[42],主要对应于岩相组合 C。阿参1井下部粗碎屑沉积段为颗粒支撑,砾岩和含砾粗砂岩成分及结构成熟度低(图5a),沉积物以滚动、跳跃方式搬运^[43],说明扇体紧邻物源区,为短距离搬运快速沉积的近源沉积体系,对应扇三角洲前缘近端叠置的主河道砂体沉积特征^[44]。中部过渡到粉砂质砂体,粒度明显变细,对应扇三角洲前缘远端水下分流河道砂体,水动力逐渐减弱。泥岩中见形状不规则的粗粒砂体,砂岩中也可见垮塌泥砾(图5b~d),为深水陡坡沉积环境下砂体滑塌入海,推测为扇三角洲水下局部重力流沉积,对应前扇三角洲沉积特征。

3.2.4 障壁岛海岸成因砂体

障壁岛海岸沉积体系为海陆过渡相,由于障壁岛隔开沿岸海域与外围广海,广海一侧发育开阔陆表海,向岸一侧受潮汐作用发育潮坪—泻湖沉积体系^[45],主要对应于岩相组合 D。砂体粒度较细且为逆粒序,底平顶凸状砂体可见波痕(图6e),反映水动力

较强的潮汐和波浪联合作用环境,对应障壁岛砂体沉积特征。砂泥互层形成的波状层理、脉状层理(图6a, g)和小型羽状交错层理(图6f),反映韵律性潮汐作用。砂体粒度向上从中细砂岩到粉砂岩逐渐变细,反映潮下带至潮间带水动力逐渐减弱。双黏土层(图6b)是在潮汐作用下形成的一种标志性沉积构造,前积砂质层和黏土质泥层厚度不均,表明涨潮退潮能量不均^[46],对应潮坪沉积特征。含碳泥岩层面见黄铁矿及完整的植物叶片(图6c, d),反映还原闭塞的静水沉积环境,对应潟湖沉积特征。

3.2.5 无障壁海岸砂体

无障壁海岸位于与大洋连通性好的海岸地带,与广海陆棚之间没有被障壁岛、滩,或生物礁隔开,海岸受较明显的波浪及沿岸流的作用,海水可以充分流通和循环^[47],主要对应于岩相组合 E。砂体粒度粗,砾岩、砂砾岩与含砾粗砂岩中石英含量极高(图7a, b),发育低角度及冲洗交错层理(图7c),反映水动力较强的海浪冲刷及波浪淘洗沉积环境,对应滨岸砂体沉积特征^[48]。泥质含量增高,说明受波浪作用影响小,对应浅水—半深水陆棚沉积特征^[49]。

3.2.6 重力流砂体

滑塌重力流沉积具有砂泥变形构造,同沉积微断层,泥质撕裂屑、不规则接触面等典型的塑性变形构造^[50-52],主要对应于岩相组合 F。砂岩与泥岩呈突变接触,接触面不规则,可见大量层间揉皱变形(图8a),阶梯状小断层错断内部弱固结的砂泥纹层(图8b),反映其处于快速沉积的半固结状态。磨圆较好

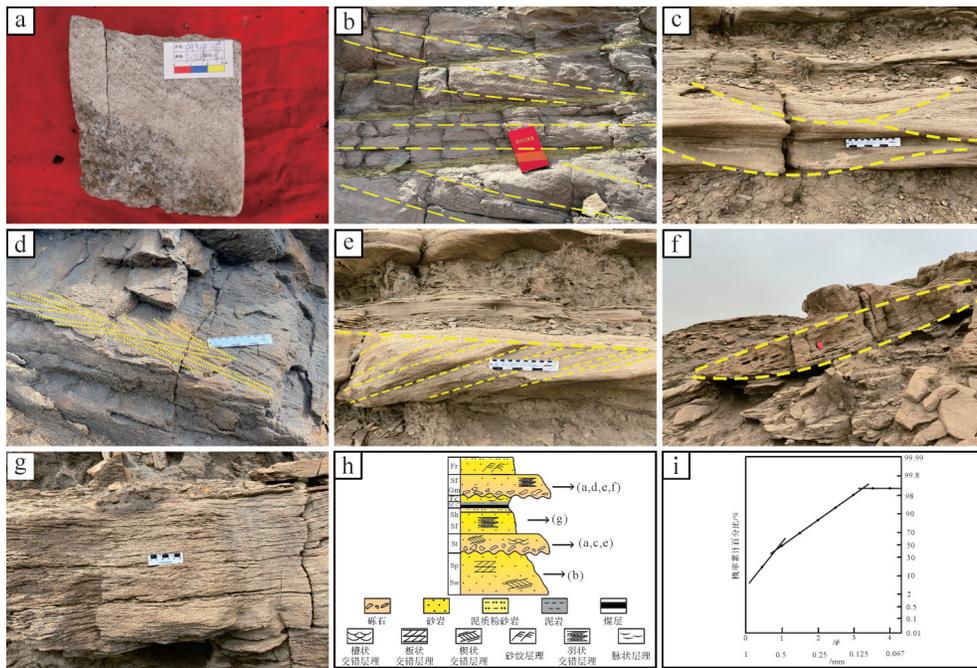


图4 鄂尔多斯盆地西缘羊虎沟组岩相组合B沉积特征

(a)灰白色粗砂岩,板状交错层理,羊二段,阿参1井,3 277.79 m;(b)羊虎沟组中砂岩潮汐砂脊前积层理,层间夹泥质披盖层,下河沿;(c)羊虎沟组槽状交错层理,呼鲁斯太;(d)羊虎沟组羽状交错层理,乌达;(e)羊虎沟组楔状交错层理,呼鲁斯太;(f)羊虎沟组潮道砂,呼鲁斯太;(g)羊虎沟组砂坪脉状层理,乌达;(h)岩相组合B综合柱状剖面示意图;(i)潮控三角洲潮汐砂脊砂岩粒度分布概率曲线图,李31井,4 038.00 m

Fig.4 Sedimentary characteristics of lithofacies association B from the Yanghugou Formation, western Ordos Basin

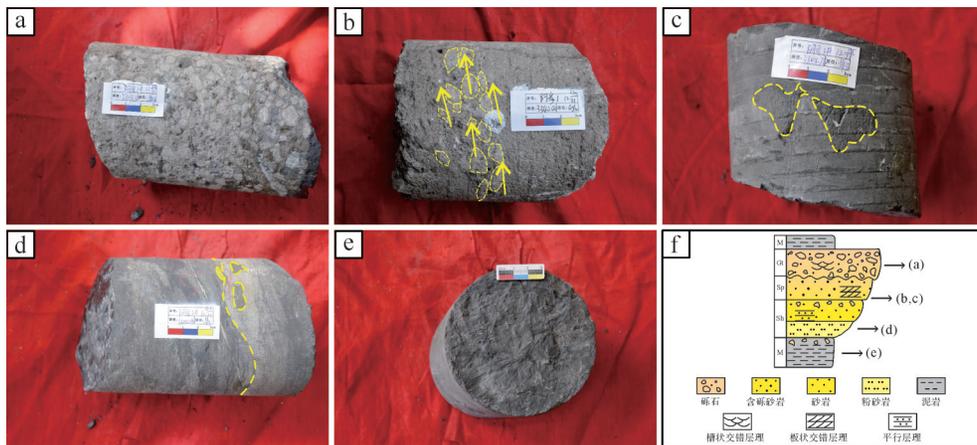


图5 鄂尔多斯盆地西缘羊虎沟组岩相组合C沉积特征

(a)灰白色石英砾岩,羊三段,阿参1井,3 343.32 m;(b)浅灰色含砾粗砂岩,砾石具定向性,羊三段,阿参1井,3 340.00 m;(c)灰黑色泥岩夹粗粒砂体,羊三段,阿参1井,3 345.78 m;(d)灰黑色粉砂岩、泥岩垮塌进入砂岩,羊三段,阿参1井,3 345.16 m;(e)植物化石,羊三段,阿参1井,3 345.78 m;(f)岩相组合C综合柱状剖面示意图

Fig.5 Sedimentary characteristics of lithofacies association C from the Yanghugou Formation, western Ordos Basin

的砂砾、泥砾(图8c)和棱角尖锐呈撕裂状的泥质撕裂屑(图8d)分散在粉砂岩中,具定向性,推测为沉积物重力失稳后发生快速滑塌,砂砾表面圆滑,在滑塌后可能发生了流动搬运^[53]。砂体整体呈块状发生滑动滑塌进入泥岩中(图8e),反映稳定深水且沉积坡度较大的沉积环境,对应滑塌重力流沉积特征^[54]。

4 沉积砂体时空展布

4.1 沉积相演化

根据对研究区野外露头剖面、岩心观察和钻井资料分析,选取平面上分布均匀、层位较全的巴参2井、苏峪口、呼鲁斯太等11处钻井及剖面(连井平面

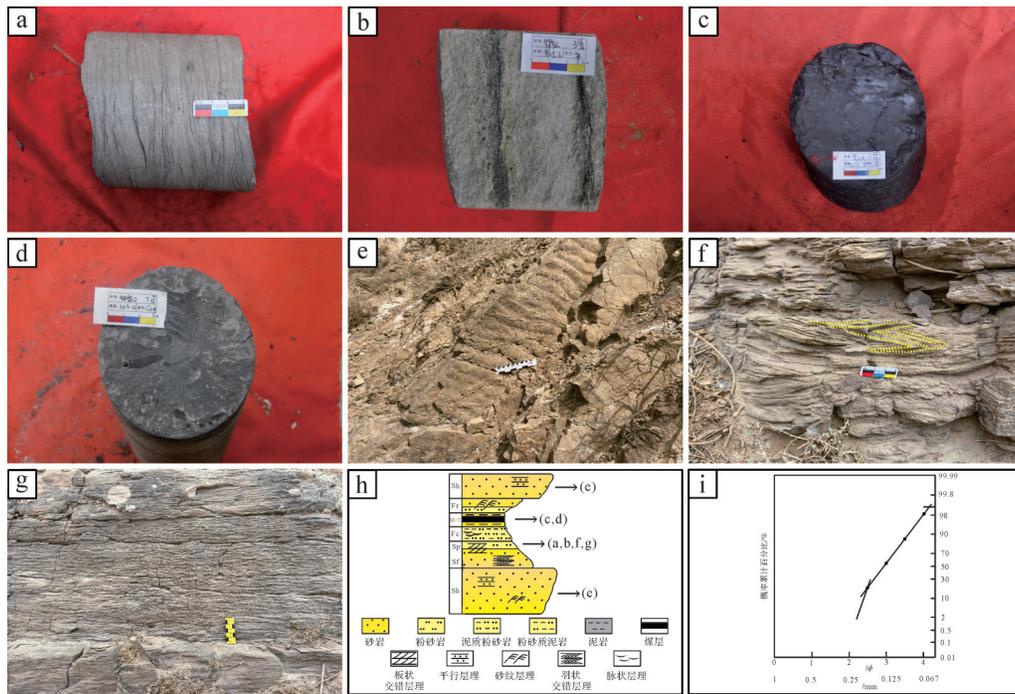


图6 鄂尔多斯盆地西缘羊虎沟组岩相组合D沉积特征

(a)羊虎沟组细砂岩,脉状层理,巴参2井,3 210.95 m;(b)羊虎沟组双黏土层,鄂32井,3 905.20 m;(c)羊虎沟组黑色泥岩,黄铁矿,忠6井,2 617.30 m;(d)羊虎沟组泥质粉砂岩,植物叶片,银探2井,2 570.52 m;(e)羊虎沟组波痕,小洪沟;(f)羊虎沟组羽状交错层理,土坡;(g)羊虎沟组脉状层理,土坡;(h)岩相组合D综合柱状剖面示意图;(i)障壁海岸潮坪砂岩粒度概率曲线图,图东4井

Fig.6 Sedimentary characteristics of lithofacies association D from the Yanghugou Formation, western Ordos Basin

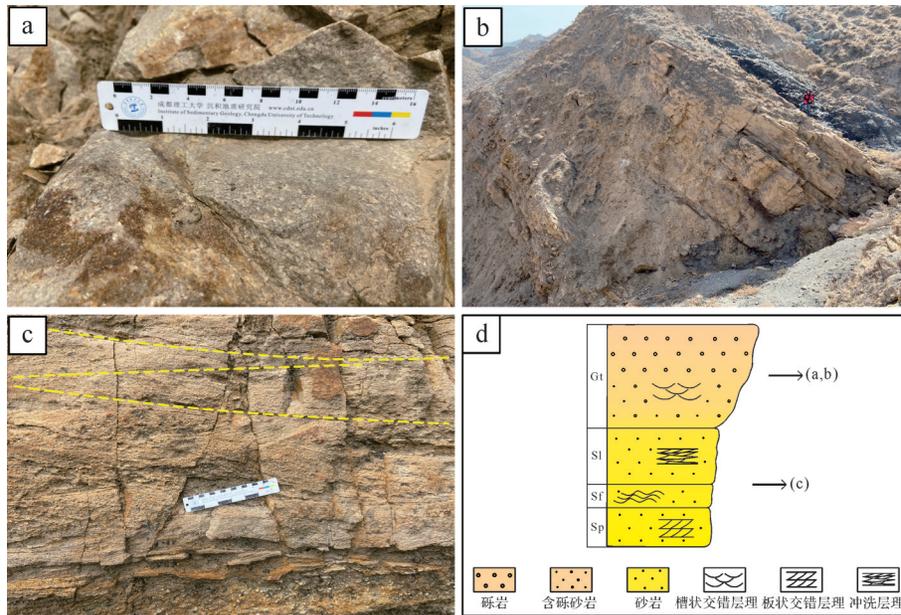


图7 鄂尔多斯盆地西缘羊虎沟组岩相组合E沉积特征

(a)羊虎沟组底部滨岸相纯石英砾岩,小洪沟;(b)羊虎沟组灰色含砾砂岩,下河沿;(c)羊虎沟组低角度冲交错层理,乌达;(d)岩相组合E综合柱状剖面示意图

Fig.7 Sedimentary characteristics of lithofacies association E from the Yanghugou Formation, western Ordos Basin

位置见图1b),进行综合地层划分对比。

由北侧东西向沉积相对比剖面图(图9)可以看出,羊虎沟期地层厚度有明显差异,整体呈“东厚西薄”的特点,在呼鲁斯太处达到最深,厚约700 m,鄂16

井沉积厚度较薄,不足40 m,东部砂体发育程度优于西部砂体。羊三段至羊二段砂体横向上连续性差,但砂体沉积厚度较大,发育潮控三角洲沉积体系的潮汐砂脊砂体。羊一段地层厚度及砂体厚度较小,

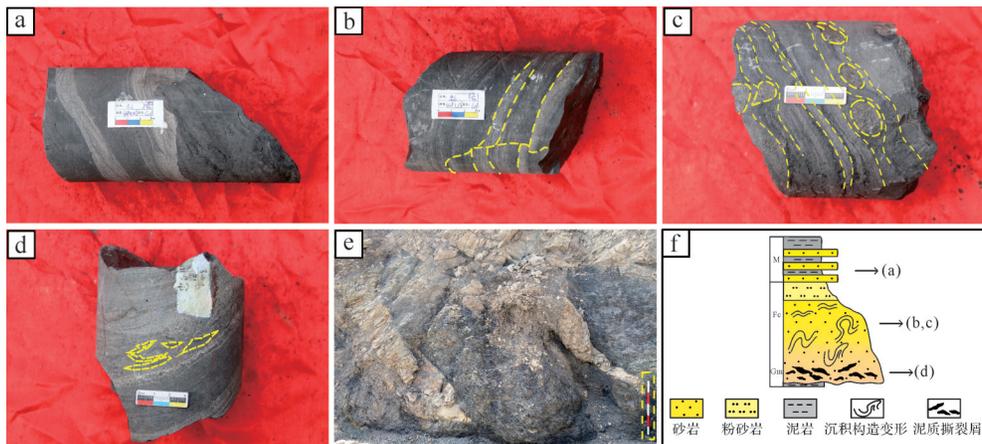


图8 鄂尔多斯盆地西缘羊虎沟组岩相组合F沉积特征

(a)重力流成因垮塌泥砾,砂纹交错层理,羊二段,忠6井,4 394.06 m;(b)羊虎沟组泥质粉细砂岩,同沉积变形,忠6井,4 391.23 m;(c)羊虎沟组重力流成因垮塌泥砾,忠6井,4 396.73 m;(d)羊虎沟组定向泥质撕裂屑,忠6井,4 393.24 m;(e)羊虎沟组重力流砂体,下河沿;(f)岩相组合F综合柱状剖面示意图

Fig.8 Sedimentary characteristics of lithofacies association F from the Yanghugou Formation, western Ordos Basin

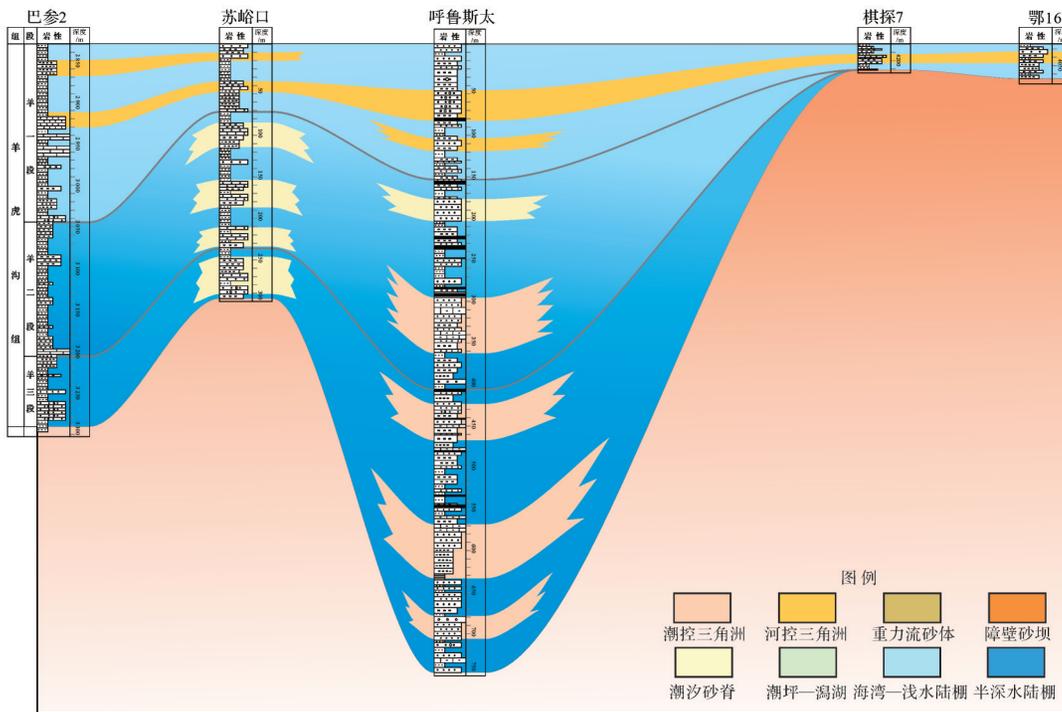


图9 鄂尔多斯盆地西缘羊虎沟组东西向沉积相对比剖面图(北侧A—A')

Fig.9 East-west sedimentary contrast profile of the Yanghugou Formation in the western margin of the Ordos Basin (north side A—A')

在东西向上连通性较好,沉积环境与物源供给较稳定,具有填平补齐特征,发育河控三角洲沉积砂体。该剖面表明羊虎沟组整体在纵向上具有水体由深变浅的特征。

南侧东西向沉积相对比剖面图(图10)表明羊虎沟组受中央古隆起影响,仍呈“东厚西薄”的特点,地层厚度较北部有所增加,在韦参1井处达到最深,厚

约650 m,李64井处沉积厚度较薄,厚约30 m。该对比剖面揭示砂体横向上连续性差,韦参1井处羊二段单个砂体沉积厚度较大。羊三段至羊二段东侧发育障壁砂坝和少量重力流砂体,西侧地势较陡,发育大量重力流成因砂体。羊一段东侧发育河控三角洲沉积砂体,西侧发育障壁海岸沉积体系中的障壁岛砂体。该剖面在纵向上仍具有水体由深变浅的特征。

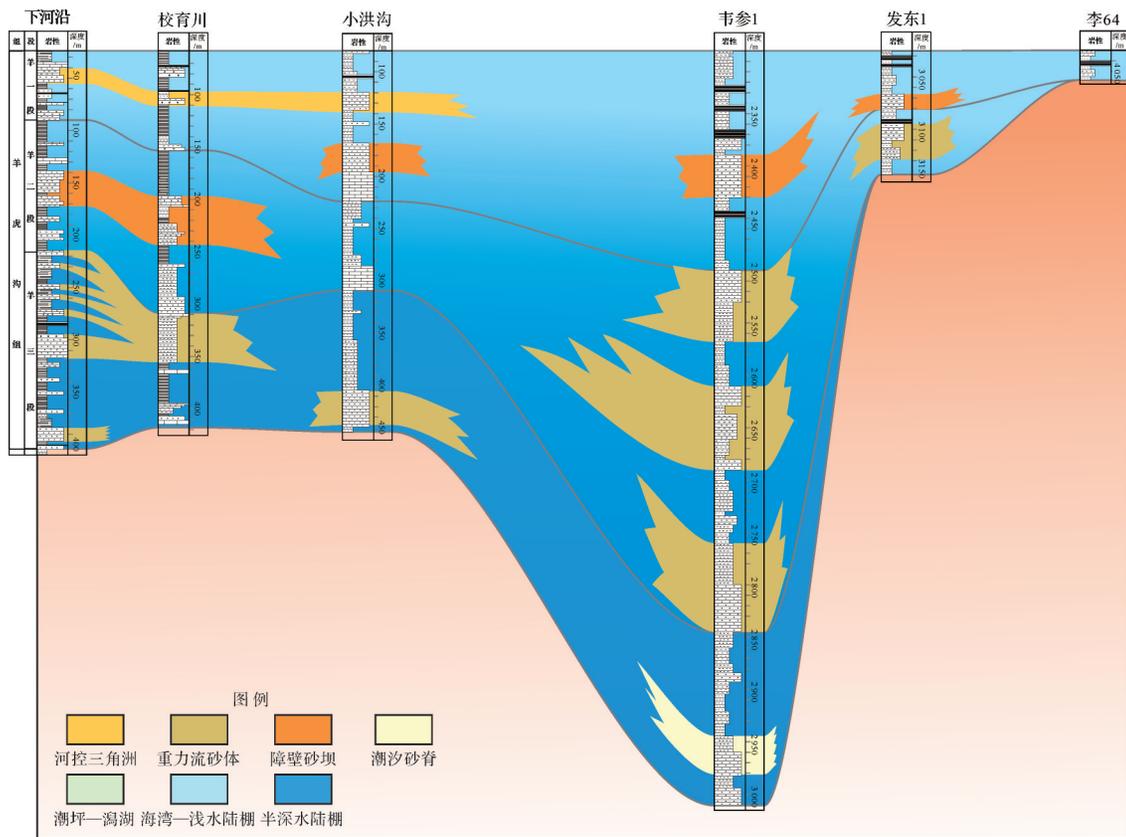


图 10 鄂尔多斯盆地西缘羊虎沟组东西向沉积相对比剖面图(南侧 B—B')

Fig.10 East-west sedimentary contrast section of the Yanghugou Formation in the western margin of the Ordos Basin (south side B-B')

4.2 沉积砂体展布

4.2.1 羊三段沉积期

羊三段沉积时期,整体地层沉积特征呈由北向南的“喇叭口”形,研究区主要发育南北两个沉降中心,北部位于呼鲁斯太—乌达一带,为一个狭窄的沉积区,最大厚度约为 200 m,砂体集中分布于此。南部沉降中心位于大石头井沟—中卫地区,最大厚度约为 400 m,砂体主要位于该沉降中心南侧高部位。

研究区东北部发育潮控三角洲沉降体系,受潮汐作用影响,砂体主要为潮道、潮坪和潮汐砂脊,最大砂厚约 90 m。垂向上潮坪砂质含量高,夹于潮道间,平面上潮汐砂脊砂体形态为典型裂指状,从河口处向海洋方向放射状分布,中部地区零星可见平行中央古隆起的潮汐砂脊砂体,呈北东—南西向展布。西北部阿参 1 井地区发育扇三角洲,整体粒度较粗,河流作用为主使其平面形态呈扇形,砂厚约 60 m,垂向上具向上粒度变粗的逆粒序结构特征。南部砂体整体表现为无障壁海岸沉积,展布方向与海岸线大致平行,下

河沿地区局部可见重力流沉积砂体(图 11)。

4.2.2 羊二段沉积期

羊二段沉积时期,地层沉积范围扩大,北部沉降中心向南迁移至石嘴山东部,最大厚度约为 300 m;南部沉降中心依然位于大石头井沟—中卫地区,厚度增加到 500 m。相对于羊三段沉积期,该时期地层厚度增加,沉降面积扩大,南北砂体展布面积增大,并逐渐向东超覆。

研究区北部受潮汐作用影响的范围增大,潮汐砂脊沉积砂体最远可延伸至银川以南地区。潮汐砂脊平面上为北东—南西方向展布,单个砂体平行于中央古隆起边界,厚度变化大,整体厚度 10~90 m 不等。土坡—大石头井沟一带发育重力流沉积,校育川地区也局部可见,发育丰富的同沉积构造变形沉积特征。南部开始发育河控三角洲,中卫、小洪沟局部地区可见透镜状障壁沙坝。中央古隆起西侧潮汐砂脊被逐渐改造为小型障壁岛,东部高部位逐渐开始发育潮坪—潟湖沉积砂体(图 12)。

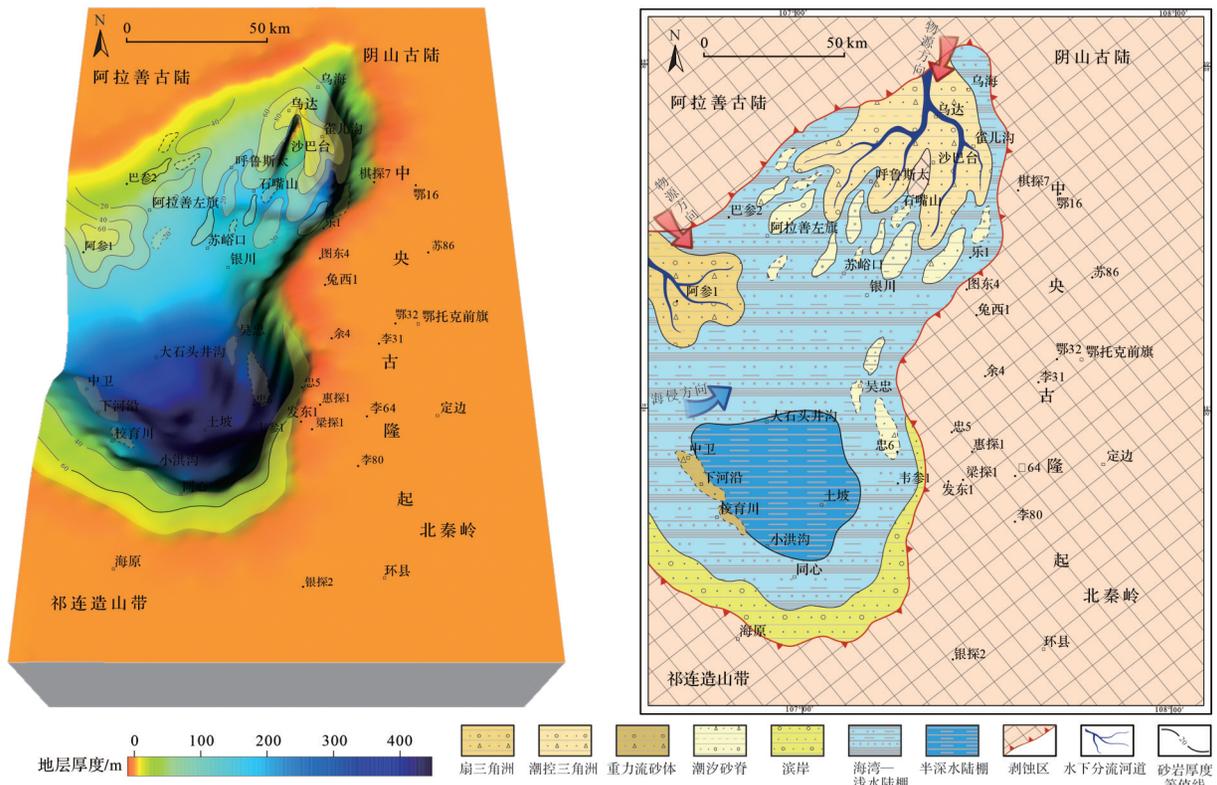


图 11 鄂尔多斯盆地西缘羊虎沟组羊三段沉积期砂体展布及沉积相

Fig.11 Sand body distribution and sedimentary facies for the 3rd member of Yanghugou Formation, western Ordos Basin

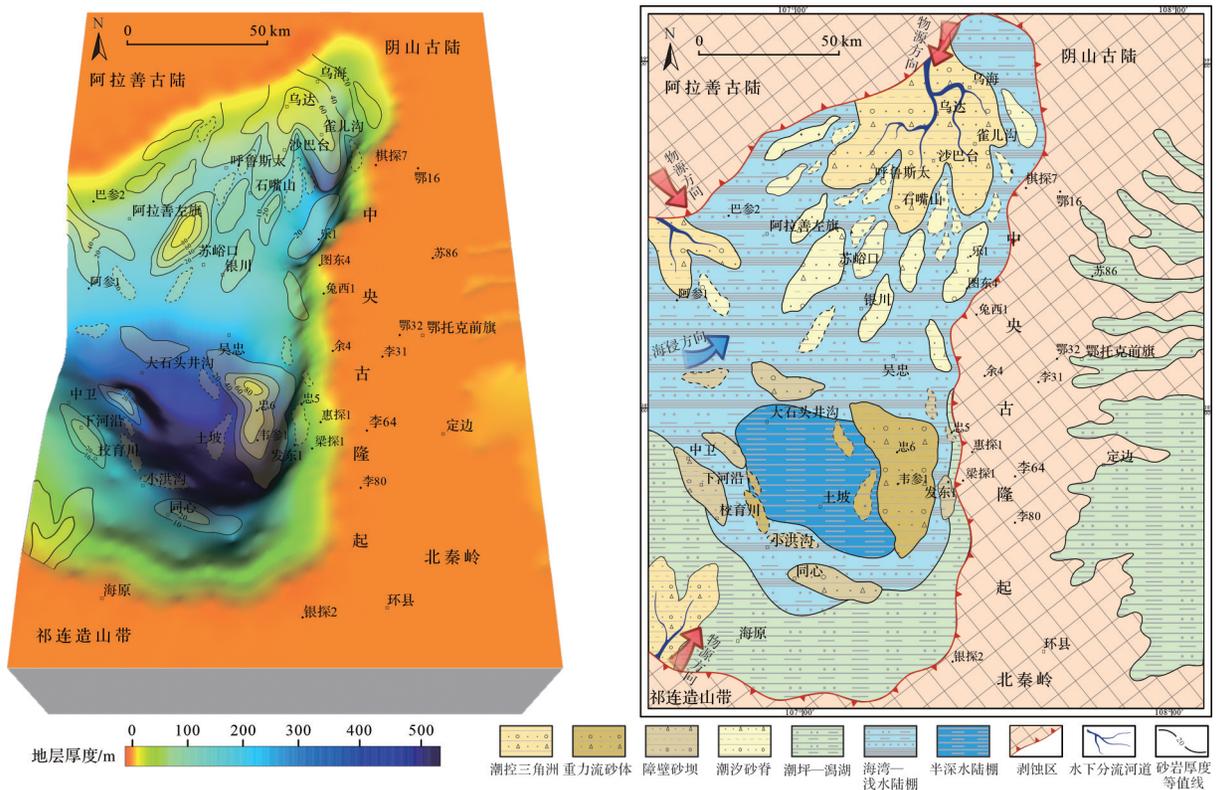


图 12 鄂尔多斯盆地西缘羊虎沟组羊二段沉积期砂体展布及沉积相

Fig.12 Sand body distribution and sedimentary facies for the 2nd member of the Yanghugou Formation, western Ordos Basin

4.2.3 羊一段沉积期

羊一段沉积时期,地层沉积范围进一步扩大,北部沉降中心逐渐填平补齐,南部沉降中心继续向北迁移至吴忠地区,最大厚度约为200 m。相较羊三、羊二段沉积期,地层沉积厚度减小,但沉积范围大面积扩大,研究区沉积砂体逐渐东西连片。

研究区北部三角洲转变为河控三角洲沉积体系,砂体形态为向海突出的朵体,砂厚小于50 m,推进至银川附近。南部河控三角洲砂体向北推进至下河沿地区。研究区中央古隆起西侧的潮汐砂脊被逐渐改造为障壁岛砂体,砂厚10~30 m。被改造形成的障壁岛砂体平面上呈北东—南西方向展布,障壁岛以东则整体为潮坪—泻湖沉积。中央古隆起此时变为水下低凸起,对砂体的阻隔作用变弱致使西缘沉积体系与东部相连(图13)。

5 控制因素

鄂尔多斯盆地西缘地区为克拉通边缘裂陷盆地,该类盆地的砂体沉积通常受控于构造、古地貌、物源及海平面等因素^[55]。西缘及邻区为裂陷海湾背景,具有弱物源、强构造的特征,构造活动控制着研

究区物源供给差异与沉积充填演化过程^[56-57]。鄂尔多斯盆地西缘及邻区在漫长的构造演化过程中形成中央古隆起与裂陷等构造单元^[20-21],决定了研究区古地貌格局,而构造运动影响下的古地貌往往控制着物源通道的分布和砂体的汇聚方向^[58]。不同物源区的构造背景差异决定了其供源能力的强弱,从而制约着盆内的砂体展布与源—汇系统分异特征^[59]。此外,构造演化驱动下的海平面升降影响可容纳空间的改变,控制了不同时期砂体的发育特征^[57]。

5.1 构造—古地貌

研究区羊虎沟组时期,沉积盆地整体呈“喇叭口”形,受裂陷海湾水进水退影响和东部中央古隆起的障蔽作用,沉积相带大致呈北东—南西方向展布。北部紧邻阿拉善—阴山古陆,由于构造活动强烈,地势较陡;南部与秦岭—祁连造山带相连,构造相对较弱,地势低缓。

研究区内羊三段沉积时期为裂陷初期,盆地整体狭窄。东北部水下低凸起两侧低地貌成为砂体运移的通道,控制砂体沉积过程,中央古隆起分割祁连海和华北海,阻挡了砂体向东的运移。由于北部构

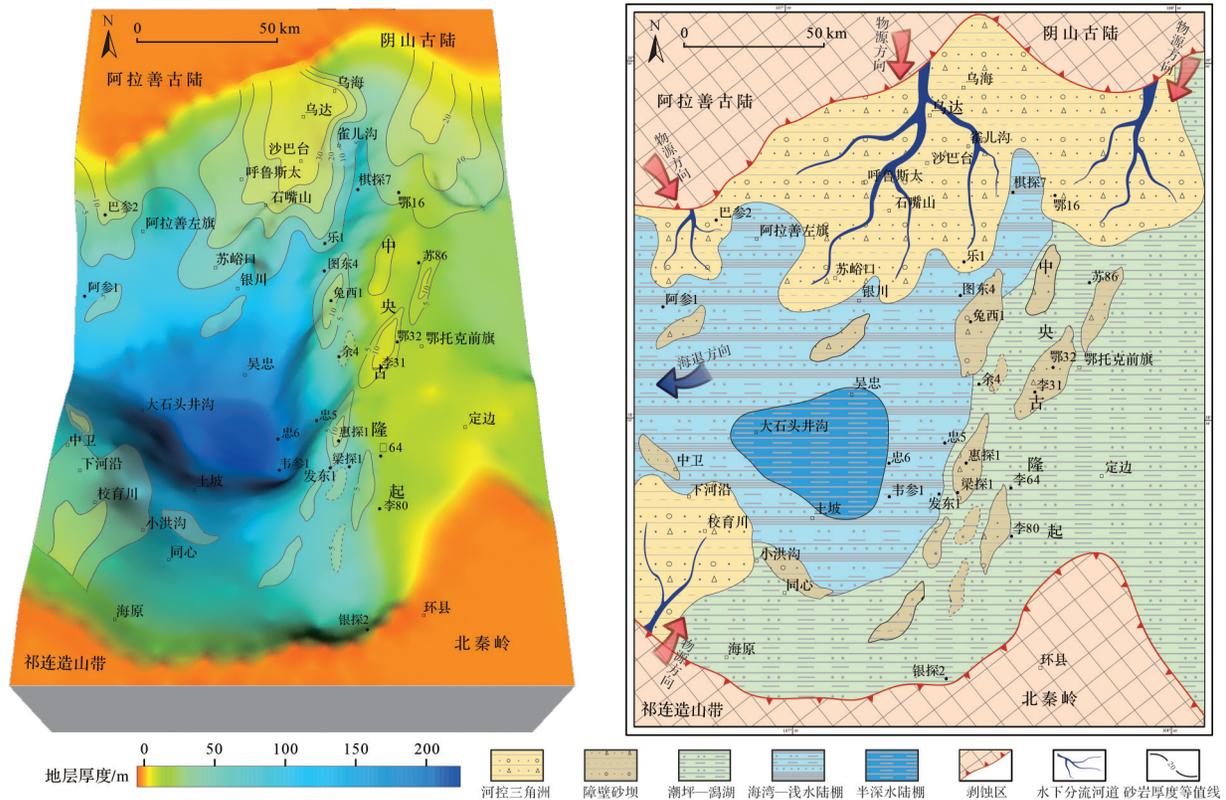


图13 鄂尔多斯盆地西缘羊虎沟组羊一段沉积期砂体展布及沉积相

Fig.13 Sand body distribution and sedimentary facies for the 1st member of the Yanghugou Formation, western Ordos Basin

造活动强烈,且临近物源区,河流携带粗粒沉积物在陡坡部位快速堆积形成扇三角洲。南部构造活动较弱,无明显输砂体系,则表现为无障壁海岸沉积。

羊二段沉积时期为裂陷高潮期,海侵范围扩大,潮汐作用增强,潮控三角洲沉积砂体受潮汐作用改造强烈。构造活动导致盆地地势高差大^[60],土坡一大石头井沟区域深水斜坡环境下发育滑塌重力流沉积。鄂托克旗一定边地区砂体发育在中央古隆起之上相对高部位,可容纳空间较小,发育潮坪沉积砂体。

羊一段沉积时期,构造活动减弱,沉积环境稳定且水体变浅,河流搬运占主导作用。羊三、羊二沉积期形成的潮控三角洲逐渐转变为大面积连片发育的河控三角洲沉积。三角洲前缘水下分流河道和河口坝成因砂体,由于地貌减缓、可容纳空间的降低,向前进积至盆地沉积中心附近。中央古隆起主体位于水下,对砂体的控制作用逐渐减弱,发育东西连片的障壁岛和潮坪—潟湖沉积。

5.2 物源

物源方向决定了盆地内部三角洲相砂体的发育位置与推进方向^[57],对整个盆地的沉积作用和构造演化等方面意义重大^[5]。研究区北部砂体主要来自北部的阴山古陆、西北缘的阿拉善古陆,南部砂体则主要来自秦岭—祁连造山带^[27],其中北部物源是控制区内羊虎沟组砂体沉积的最主要物源^[61]。

羊虎沟组沉积时期,鄂尔多斯盆地西缘整体为北东—南西方向供源,北部物源供给相对较强^[29]。晚古生代早—中期,华北板块大面积隆升,古阴山褶皱造山带形成,产生物源供给区^[28,61]。早石炭世,阿拉善地块开始遭受海侵,阿拉善古陆隆升后物源供给比较稳定^[62],与阴山古陆物源在呼鲁斯太地区汇合并共同向南继续推进。羊虎沟组沉积时期北秦岭构造带与华北板块南缘发生碰撞,是南部物源体系的重要组成部分^[29],研究区西南部开始发育小型河控三角洲砂体。随着物源供给进一步增强,研究区北部和南部河控三角洲砂体大面积发育。

5.3 气候与海平面

研究区在羊虎沟组沉积期总体气候温暖潮湿^[14],一年四季降雨充沛,为海陆交互相沉积建造^[17],水系分布广泛,形成大量中—小型三角洲沉积体系和障壁海岸沉积体系。研究区羊虎沟组沉积期的海平面变化为一套完整的海进海退旋回,羊一段沉积时期为大面积的海退期^[63]。羊三段沉积时期海平面总体

上升,可容纳空间较高^[64],较低的输砂速率,致使盆地三角洲朵体较小,且容易受到潮汐作用的改造。至羊二段沉积时期,海平面达到最高,可容空间快速增大,物源供给虽然增强,但总体仍表现为欠补偿背景下的边缘沉积。潮控三角洲砂体大部分位于潮间—潮下带,该时期潮汐砂脊最为发育。到羊一段沉积时期,海平面快速下降,可容空间迅速减小,砂体不断向盆地沉积中心推进^[64]。多期次三角洲前缘河道侧向迁移分布使三角洲面积逐渐扩大。

6 结论

(1) 鄂尔多斯盆地西缘及邻区羊虎沟组中可识别出6种岩相组合,对应河控三角洲、潮控三角洲、扇三角洲、障壁岛海岸、无障壁海岸和滑塌重力流6类成因机制。

(2) 羊三段沉积时期,北部发育潮控三角洲和扇三角洲砂体,潮汐砂脊从入海口向广海呈放射状分布,中部少量潮汐砂脊平行于中央古隆起,南部砂体表现为无障壁海岸沉积;羊二段沉积时期,北部潮控三角洲砂体被强烈改造,盆地中央斜坡部位发育重力流沉积,中央古隆起西侧潮汐砂脊被逐渐改造为小型障壁岛,其高部位逐渐发育潮坪—潟湖沉积,南部开始发育河控三角洲砂体;羊一段沉积时期,河流搬运占主导,研究区北部和南部潮控三角洲完全演变为河控三角洲。中央古隆起演化为水下低凸起,障壁岛有效隔绝广海与中央古隆起东侧水体,古隆起之上潮坪—潟湖沉积大面积发育且连片分布。

(3) 羊三段沉积时期为裂陷早期,狭窄的裂陷盆地制约砂体发育,该时期砂体展布主要受构造活动和潮汐作用控制;羊二段沉积时期为裂陷高潮期,海侵范围扩大,构造活动和海平面变化控制该时期的砂体沉积过程;羊一段沉积时期,构造活动减弱,中央古隆起主体位于水下,砂体东西连通。鄂尔多斯盆地西缘及邻区羊虎沟组砂体沉积过程受构造运动、古地貌演化、物源供给、古气候、海平面等多因素共同影响,但主要受控于构造活动与古地理演化。

致谢 感谢成都理工大学沉积地质研究院刘磊老师的指导,感谢成都理工大学沉积地质研究院王志伟博士和韩勇博士对本文提出的建议和帮助。各位评审专家及编辑部老师对本文提出了宝贵的修改意见,在此表示衷心的感谢!

参考文献(References)

- [1] 王崇敬,徐浩,杨光,等. 鄂尔多斯西缘羊虎沟组页岩气聚集地质条件分析[J]. 中国煤炭地质,2014,26(2):18-20,24. [Wang Chongjing, Xu Hao, Yang Guang, et al. Geological conditions of Yanghugou Formation shale gas accumulation on western margin of Ordos Basin[J]. Coal Geology of China, 2014, 26(2): 18-20, 24.]
- [2] 杨华,陶家庆,欧阳征健,等. 鄂尔多斯盆地西缘构造特征及其成因机制[J]. 西北大学学报(自然科学版),2011,41(5):863-868. [Yang Hua, Tao Jiaqing, Ouyang Zhengjian, et al. Structural characteristics and forming mechanism in the western margin of the Ordos Basin[J]. Journal of Northwest University (Natural Science Edition), 2011, 41(5): 863-868.]
- [3] 朱昊. 鄂尔多斯盆地西缘中南段地质结构及其形成演化[D]. 北京:中国地质大学(北京),2015:1-133. [Zhu Hao. Geologic structure and evolution of the south-central segments of west Ordos Basin[D]. Beijing: China University of Geosciences (Beijing), 2015: 1-133.]
- [4] 王子腾,王康乐,王峰,等. 鄂尔多斯盆地西缘羊虎沟组物源区分析[J]. 地球科学与环境学报,2019,41(3):281-296. [Wang Ziteng, Wang Kangle, Wang Feng, et al. Provenance analysis of Yanghugou Formation in the western margin of Ordos Basin, China[J]. Journal of Earth Sciences and Environment, 2019, 41(3): 281-296.]
- [5] 赵红格. 鄂尔多斯盆地西部构造特征及演化[D]. 西安:西北大学,2003:1-133. [Zhao Hongge. Structural characteristics and the evolution in western Ordos Basin[D]. Xi'an: Northwest University, 2003: 1-133.]
- [6] 赵红格,刘池洋,王峰,等. 鄂尔多斯盆地西缘构造分区及其特征[J]. 石油与天然气地质,2006,27(2):173-179. [Zhao Hongge, Liu Chiyang, Wang Feng, et al. Structural division and characteristics in western edge of Ordos Basin[J]. Oil & Gas Geology, 2006, 27(2): 173-179.]
- [7] 王碧涛,曹丽,李化斌,等. 鄂尔多斯盆地西缘断褶带成藏富集规律研究[J]. 石油化工应用,2013,32(9):82-83,90. [Wang Bitao, Cao Li, Li Huabin, et al. Erdos Basin west margin fault fold belt accumulation study[J]. Petrochemical Industry Application, 2013, 32(9): 82-83, 90.]
- [8] 高春云. 鄂尔多斯盆地西缘南段构造特征及演化研究[D]. 西安:西北大学,2020:1-153. [Gao Chunyun. Research on the characteristics of structure and tectonic evolution of southern section of western margin of Ordos Basin[D]. Xi'an: Northwest University, 2020: 1-153.]
- [9] 郭宏伟,戴明建. 鄂尔多斯盆地西缘逆冲构造带对岩性岩相及水动力条件的影响[J]. 重庆科技学院学报(自然科学版),2012,14(2):15-17,77. [Guo Hongwei, Dai Mingjian. On the influence of the thrust belt to the lithology and lithofacies and the hydrodynamic conditions in western margin of Ordos Basin[J]. Journal of Chongqing University of Science and Technology (Natural Sciences Edition), 2012, 14(2): 15-17, 77.]
- [10] 张晓莉. 鄂尔多斯盆地中部上古生界沉积相演化[J]. 地球科学与环境学报,2005,27(3):26-29,37. [Zhang Xiaoli. Sedimentary facies evolution of Upper Palaeozoic formation in Ordos Basin[J]. Journal of Earth Sciences and Environment, 2005, 27(3): 26-29, 37.]
- [11] 高志东. 鄂尔多斯盆地上石炭统本溪组物源分析及有利砂体发育规律[D]. 成都:成都理工大学,2019:1-71. [Gao Zhidong. Provenance analysis of Benxi Formation of Upper Carboniferous in Ordos Basin and distribution regularity of favorable sand bodies[D]. Chengdu: Chengdu University of Technology, 2019: 1-71.]
- [12] 李斌. 鄂尔多斯盆地西部冲断带构造与控油气因素研究[D]. 西安:西北大学,2019:1-85. [Li Bin. Thrust structure and its effect on hydrocarbon in the western margin of Ordos Basin[D]. Xi'an: Northwest University, 2019: 1-85.]
- [13] 林进,李云,何剑. 鄂尔多斯延长探区本溪组物源及沉积体系分析[J]. 中国地质,2013,40(5):1542-1551. [Lin Jin, Li Yun, He Jian. An analysis of the source and the sedimentary system of the Carboniferous Benxi Formation in Yanchang area of Ordos Basin[J]. Geology in China, 2013, 40(5): 1542-1551.]
- [14] 冯凯龙,田景春,王峰,等. 鄂尔多斯盆地西缘地区羊虎沟组沉积相类型及岩相古地理演化[C]//第十五届全国古地理学及沉积学学术会议摘要集. 成都:中国矿物岩石地球化学学会岩相古地理专业委员会,2018. [Feng Kailong, Tian Jingchun, Wang Feng, et al. Sedimentary facies types and lithofacies paleogeographical evolution of the Yanghugou Formation in the western margin of Ordos Basin[C]//Abstracts of the 15th national conference on paleogeography and sedimentology. Chengdu: Professional Committee of Lithofacies Paleogeography, Chinese Society of Mineral and Rock Geochemistry, 2018.]
- [15] 侯云东,陈安清,赵伟波,等. 鄂尔多斯盆地本溪组潮汐—三角洲复合砂体沉积环境[J]. 成都理工大学学报(自然科学版),2018,45(4):393-401. [Hou Yundong, Chen Anqing, Zhao Weibo, et al. Analysis on the depositional environment of Carboniferous Benxi Formation tidal-delta sand body complex, Ordos Basin, China[J]. Journal of Chengdu University of Technology (Science & Technology Edition), 2018, 45(4): 393-401.]
- [16] 王子腾. 鄂尔多斯盆地西缘羊虎沟组物源分析与沉积特征研究[D]. 成都:成都理工大学,2020:1-83. [Wang Ziteng. Provenance analysis and sedimentary characteristics of Yanghugou Formation in the western margin of the Ordos Basin[D]. Chengdu: Chengdu University of Technology, 2020: 1-83.]
- [17] 冯娟萍,欧阳征健,陈全红,等. 鄂尔多斯盆地及周缘地区上石炭统沉积特征[J]. 古地学报,2021,23(1):53-64. [Feng Juanping, Ouyang Zhengjian, Chen Quanhong, et al. Sedimentary characteristics of the Upper Carboniferous in Ordos Basin and its adjacent areas[J]. Journal of Palaeogeography, 2021, 23(1): 53-64.]

- (1): 53-64.]
- [18] Li S Z, Jahn B M, Zhao S J, et al. Triassic southeastward subduction of North China Block to South China Block: Insights from new geological, geophysical and geochemical data [J]. *Earth-Science Reviews*, 2017, 166: 270-285.
- [19] Zhao J F, Zhou Y J, Wang K, et al. Provenance and paleogeography of Carboniferous-Permian strata in the Bayanhot Basin: Constraints from sedimentary records and detrital zircon geochronology [J]. *Geoscience Frontiers*, 2021, 12 (3) : 101088.
- [20] 王治平, 全秋琦. 中国石炭—二叠纪古气候及其对板块构造的验证[J]. *地层学杂志*, 1992, 16(1): 1-11. [Wang Zhiping, Quan Qiuqi. China Carboniferous-Permian paleoclimate and its verification of plate tectonics [J]. *Journal of Stratigraphy*, 1992, 16(1): 1-11.]
- [21] 张成弓. 鄂尔多斯盆地早古生代中央古隆起形成演化与物质聚集分布规律[D]. 成都: 成都理工大学, 2013: 1-114. [Zhang Chengong. Forming evolution and sediments accumulation & distribution regularity of central paleoplift in Eopaleozoic, Ordos Basin [D]. Chengdu: Chengdu University of Technology, 2013: 1-114.]
- [22] 赵重远. 华北克拉通盆地天然气赋存的地质背景[J]. *地球科学进展*, 1990, 5 (2) : 40-42. [Zhao Chongyuan. Geological background of natural gas occurrence in North China Craton basin [J]. *Advance in Earth Sciences*, 1990, 5(2): 40-42.]
- [23] 林畅松, 张燕梅. 拉伸盆地模拟理论基础与新进展[J]. *地学前缘*, 1995, 2 (3/4) : 79-88. [Lin Changsong, Zhang Yanmei. Quantitative stretching models and computer simulation of rift basin [J]. *Earth Science Frontiers*, 1995, 2(3/4): 79-88.]
- [24] Xu S M, Feng H W, Li S Z, et al. Closure time in the East Qilian Ocean and Early Paleozoic ocean-continent configuration in the Helan Mountains and adjacent regions, NW China [J]. *Journal of Asian Earth Sciences*, 2015, 113: 575-588.
- [25] 闫建成. 鄂尔多斯盆地东部本溪组气藏地质特征[J]. *云南化工*, 2018, 45(9): 163-164. [Yan Jiancheng. Geological characteristics of the Benxi Formation gas reservoir in the eastern Ordos Basin [J]. *Yunnan Chemical Technology*, 2018, 45 (9) : 163-164.]
- [26] 符俊辉, 于芬玲. 贺兰山北段呼鲁斯太石炭纪羊虎沟组的牙形刺[J]. *古生物学报*, 1998, 37(4): 489-895. [Fu Junhui, Yu Fenling. Late Carboniferous conodonts from the Yanghugou Formation in Helanshan district, North China [J]. *Acta Palaeontologica Sinica*, 1998, 37(4): 489-895.]
- [27] 杨涛, 曹涛涛, 刘虎, 等. 武威盆地上石炭统羊虎沟组页岩气成藏条件[J]. *地质科技情报*, 2019, 38(3): 188-198. [Yang Tao, Cao Taotao, Liu Hu, et al. Shale gas accumulation condition of the Upper Carboniferous Yanghugou Formation in Wuwei Basin [J]. *Geological Science and Technology Information*, 2019, 38(3): 188-198.]
- [28] 汪正江, 张锦泉, 陈洪德. 鄂尔多斯盆地晚古生代陆源碎屑沉积源区分析[J]. *成都理工学院学报*, 2001, 28(1): 7-12. [Wang Zhengjiang, Zhang Jingquan, Chen Hongde. Study of the dispositional provenance of the terrigenous detritus in Ordos Basin in Late Paleozoic era [J]. *Journal of Chengdu University of Technology*, 2001, 28(1): 7-12.]
- [29] 陈全红, 李文厚, 刘昊伟, 等. 鄂尔多斯盆地上石炭统一中二叠统砂岩物源分析[J]. *古地理学报*, 2009, 11(6): 629-640. [Chen Quanhong, Li Wenhong, Liu Haowei, et al. Provenance analysis of sandstone of the Upper Carboniferous to Middle Permian in Ordos Basin [J]. *Journal of Palaeogeography*, 2009, 11(6): 629-640.]
- [30] 贾浪波, 钟大康, 孙海涛, 等. 鄂尔多斯盆地本溪组沉积物物源探讨及其构造意义[J]. *沉积学报*, 2019, 37(5): 1087-1103. [Jia Langbo, Zhong Dakang, Sun Haitao, et al. Sediment provenance analysis and tectonic implication of the Benxi Formation, Ordos Basin [J]. *Acta Sedimentologica Sinica*, 2019, 37 (5) : 1087-1103.]
- [31] 曹杨春. 鄂尔多斯盆地陇东地区上古生界盒8段沉积相及砂体展布规律研究[D]. 成都: 成都理工大学, 2020: 1-74. [Cao Yangchun. Study on sedimentary facies and sand body distribution rules of He 8 member of the Upper Paleozoic Hedong Formation in Longdong area of Ordos Basin [D]. Chengdu: Chengdu University of Technology, 2020: 1-74.]
- [32] 蒋子文. 鄂尔多斯盆地南部上古生界山1—盒8段物源分析及盆地耦合关系研究[D]. 西安: 西北大学, 2020: 1-238. [Jiang Ziwen. The study of provenance and basin mountain coupling of Shan1-H8 member, Upper Palaeozoic, southern Ordos Basin [D]. Xi'an: Northwest University, 2020: 1-238.]
- [33] 肖红平. 鄂尔多斯盆地山西组: 盒8段沉积体系与有利储层研究[D]. 北京: 中国地质大学(北京), 2020: 1-189. [Xiao Hongping. Depositional system and favorable reservoir of Shanxi Formation-He 8 member in Ordos Basin [D]. Beijing: China University of Geosciences (Beijing), 2020: 1-189.]
- [34] Zhang J, Zhang B H, Zhao H. Timing of amalgamation of the Alxa Block and the North China Block: Constraints based on detrital zircon U-Pb ages and sedimentologic and structural evidence [J]. *Tectonophysics*, 2016, 668-669: 65-81.
- [35] Haq B U, Schutter S R. A chronology of Paleozoic sea-level changes [J]. *Science*, 2008, 322(5898): 64-68.
- [36] 弓俐. 鄂尔多斯盆地西缘地区上古生界地层及沉积相发育特征[J]. *科技经济导刊*, 2021, 29(6): 116-117. [Gong Li. Development characteristics of the Upper Paleozoic strata and sedimentary facies in the western margin of Ordos Basin [J]. *Technology and Economic Guide*, 2021, 29(6): 116-117.]
- [37] Miall A D. Architectural-element analysis: A new method of facies analysis applied to fluvial deposits [J]. *Earth-Science Reviews*, 1985, 22(4): 261-308.
- [38] 尹泽, 刘自亮, 彭楠, 等. 鄂尔多斯盆地西缘上三叠统延长组沉积相特征研究[J]. *沉积学报*, 2019, 37(1): 163-176. [Yin Ze, Liu Ziliang, Peng Nan, et al. Study on sedimentary facies

- features of the Upper Triassic Yanchang Formation, in the western margin, Ordos Basin [J]. *Acta Sedimentologica Sinica*, 2019, 37(1): 163-176.]
- [39] 陈东阳,王峰,陈洪德,等. 鄂尔多斯盆地东部府谷天生桥剖面上古生界下石盒子组8段辫状河储层构型表征[J]. 石油与天然气地质, 2019, 40(2): 335-345. [Chen Dongyang, Wang Feng, Chen Hongde, et al. Characterization of braided river reservoir architecture of the Upper Paleozoic He 8 member on Fugu Tianshengqiao outcrop, eastern Ordos Basin[J]. *Oil & Gas Geology*, 2019, 40(2): 335-345.]
- [40] 朱筱敏. 沉积岩石学[M]. 4版. 北京:石油工业出版社, 2008: 1-482. [Zhu Xiaomin. *Sedimentary petrology* [M]. 4th ed. Beijing: Petroleum Industry Press, 2008: 1-482.]
- [41] 周恩恩,牟传龙,梁薇,等. 湘西北龙山、永顺地区龙马溪组潮控三角洲沉积的发现:志留纪“雪峰隆起”形成的新证据[J]. 沉积学报, 2014, 32(3): 468-477. [Zhou Kenken, Mou Chuanlong, Liang Wei, et al. Tide-dominated deltaic deposits in Lungamachi Formation, Longshan-Yongshun regions, north-western Hunan: The initial sedimentary responses to onset of “xuefeng uplift” [J]. *Acta Sedimentologica Sinica*, 2014, 32(3): 468-477.]
- [42] Nemeč W, Steel R J. Fan deltas: Sedimentology and tectonic settings[M]. Glasgow: Blackie and Son, 1988: 1-444.
- [43] 程立华,陈世悦,吴胜和,等. 断陷盆地陡坡带扇三角洲模拟及沉积动力学分析[J]. 海洋地质与第四纪地质, 2005, 25(4): 29-34. [Cheng Lihua, Chen Shiyue, Wu Shenghe, et al. The simulation and sedimentary dynamic analysis of fan delta in the steep slope of fault basin[J]. *Marine Geology & Quaternary Geology*, 2005, 25(4): 29-34.]
- [44] 马永平,张献文,朱卡,等. 玛湖凹陷二叠系上乌尔禾组扇三角洲沉积特征及控制因素[J]. 岩性油气藏, 2021, 33(1): 57-70. [Ma Yongping, Zhang Xianwen, Zhu Ka, et al. Sedimentary characteristics and controlling factors of fan-delta of the upper Urho Formation of Permian in Mahu Sag[J]. *Lithologic Reservoirs*, 2021, 33(1): 57-70.]
- [45] 沙雪梅,梁苏娟. 陆源障壁岛砂坝有效储层综合预测技术与应用:以韦德迈阿盆地B区块泥盆系为例[J]. 天然气地球科学, 2021, 32(3): 447-456. [Sha Xuemei, Liang Sujuan. Comprehensive reservoir prediction of terrigenous barrier bar and its application: Case study of Devonian in block B, Oued Mya Basin, Algeria [J]. *Natural Gas Geoscience*, 2021, 32(3): 447-456.]
- [46] 杨建军. 潮控沉积·地震序列·前兆半月周期·调制与共振[J]. 国际地震动态, 1989(6): 11-13. [Yang Jianjun. Tidal sediment, earthquake sequence, precursory semi-monthly period, tuning and resonance[J]. *Recent Developments in World Seismology*, 1989(6): 11-13.]
- [47] 刘宝珺. 沉积岩石学[M]. 北京:地质出版社, 1980: 1-494. [Liu Baojun. *Sedimentary petrology* [M]. Beijing: Geological Publishing House, 1980: 1-494.]
- [48] 邓玄,薛国庆,王继成,等. 珠江口盆地WCA油田珠江组一段无障壁海岸相沉积特征研究[J]. 复杂油气藏, 2019, 12(4): 36-41. [Deng Xuan, Xue Guoqing, Wang Jicheng, et al. Sedimentary characteristics of wave dominated shoreline facies without barrier of the First member of Zhujiang Formation of WCA oilfield in Pearl River Mouth Basin[J]. *Complex Hydrocarbon Reservoirs*, 2019, 12(4): 36-41.]
- [49] 代云娇,杨朝强,孙艺嘉,等. 浅海陆棚相沉积特征及其沉积差异性分析:以珠江口盆地文昌A/B/C油田为例[J]. 科学技术与工程, 2016, 16(21): 193-199, 205. [Dai Yunjiao, Yang Zhaoqiang, Sun Yijia, et al. The analysis of sedimentary characteristics and sedimentary differences in neritic shelf: A case of Wenchang A/B/C district in Pearl River Mouth Basin[J]. *Science Technology and Engineering*, 2016, 16(21): 193-199, 205.]
- [50] 杨田,操应长,王艳忠,等. 深水重力流类型、沉积特征及成因机制:以济阳坳陷沙河街组三段中亚段为例[J]. 石油学报, 2015, 36(9): 1048-1059. [Yang Tian, Cao Yingchang, Wang Yanzhong, et al. Types, sedimentary characteristics and genetic mechanisms of deep-water gravity flows: A case study of the middle submember in member 3 of Shahejie Formation in Jiyang Depression [J]. *Acta Petrolei Sinica*, 2015, 36(9): 1048-1059.]
- [51] 操应长,王思佳,王艳忠,等. 滑塌型深水重力流沉积特征及沉积模式:以渤海湾盆地临南洼陷古近系沙三中亚段为例[J]. 古地理学报, 2017, 19(3): 419-432. [Cao Yingchang, Wang Sijia, Wang Yanzhong, et al. Sedimentary characteristics and depositional model of slumping deep-water gravity flow deposits: A case study from the middle member 3 of Paleogene Shahejie Formation in Linnan subsag, Bohai Bay Basin [J]. *Journal of Palaeogeography*, 2017, 19(3): 419-432.]
- [52] Shanmugam G. 50 years of the turbidite paradigm (1950s-1990s): deep-water processes and facies model: A critical perspective [J]. *Marine and Petroleum Geology*, 2000, 17(2): 285-342.
- [53] 王家豪,王华,肖敦清,等. 陆相断陷湖盆异重流与滑塌型重力流沉积辨别[J]. 石油学报, 2020, 41(4): 392-402, 411. [Wang Jiahao, Wang Hua, Xiao Dunqing, et al. Differentiation between hyperpycnal flow deposition and slump-induced gravity flow deposition in terrestrial rifted lacustrine basin [J]. *Acta Petrolei Sinica*, 2020, 41(4): 392-402, 411.]
- [54] 符勇,李忠诚,万谱,等. 三角洲前缘滑塌型重力流沉积特征及控制因素:以松辽盆地大安地区青一段为例[J]. 岩性油气藏, 2021, 33(1): 198-208. [Fu Yong, Li Zhongcheng, Wan Pu, et al. Sedimentary characteristics and controlling factors of slump gravity flow in delta front: A case study of Qing 1 member in Da'an area, Songliao Basin [J]. *Lithologic Reservoirs*, 2021, 33(1): 198-208.]
- [55] 翟咏荷,何登发,马静辉,等. 鄂尔多斯盆地及邻区晚石炭世本溪期构造:沉积环境及原型盆地特征[J]. 地质科学, 2020,

- 55(3):726-741. [Zhai Yonghe, He Dengfa, Ma Jinghui, et al. Tectonic-depositional environment and prototype basins during the depositional Period of Late Carboniferous Benxi Formation in Ordos Basin[J]. Chinese Journal of Geology, 2020, 55(3): 726-741.]
- [56] 童亨茂,孟令箭,蔡东升,等. 裂陷盆地断层的形成和演化:目标砂箱模拟实验与认识[J]. 地质学报,2009,83(6):759-774. [Tong Hengmao, Meng Lingjian, Cai Dongsheng, et al. Fault formation and evolution in rift basins: Sandbox modeling and cognition[J]. Acta Geologica Sinica, 2009, 83(6): 759-774.]
- [57] 郭军,陈洪德,王峰,等. 鄂尔多斯盆地太原组砂体展布主控因素[J]. 断块油气田,2012,19(5):568-571. [Guo Jun, Chen Hongde, Wang Feng, et al. Main controlling factors of Taiyuan Formation sand body distribution in Ordos Basin [J]. Fault-Block Oil & Gas Field, 2012, 19(5): 568-571.]
- [58] 王权,李晓红,赵璇,等. 二连盆地断陷湖盆沉积砂体分布主要控制因素[J]. 油气地质与采收率,2013,20(6):42-45,50. [Wang Quan, Li Xiaohong, Zhao Xuan, et al. Main controlling factors of sedimentary sandbodies distribution in fault sag, Erlian Basin [J]. Petroleum Geology and Recovery Efficiency, 2013, 20(6): 42-45, 50.]
- [59] 田景春,吴琦,王峰,等. 鄂尔多斯盆地地下石盒子组盒8段储集砂体发育控制因素及沉积模式研究[J]. 岩石学报,2011,27(8):2403-2412. [Tian Jingchun, Wu Qi, Wang Feng, et al. Research on development factors and the deposition model of large area reservoir sandstones of He8 section of Xiashihezi Formation of Permian in Ordos Basin [J]. Acta Petrologica Sinica, 2011, 27(8): 2403-2412.]
- [60] 王超. 浙东四明山甬江流域地貌计量指标与构造地貌研究[D]. 上海:华东师范大学,2018:1-74. [Wang Chao. Quantitative geomorphic indices characteristics and tectonics of the Yong River basin in Siming Mountain, eastern Zhejiang [D]. Shanghai: East China Normal University, 2018: 1-74.]
- [61] 赵谦平,王若谷,高飞,等. 鄂尔多斯盆地东南部延长探区上古生界物源分析[J]. 西北大学学报(自然科学版),2015,45(6):933-941. [Zhao Qianping, Wang Ruogu, Gao Fei, et al. Provenance analysis of Upper Paleozoic in Yanchang blocks, the southeast Ordos Basin [J]. Journal of Northwest University (Natural Science Edition), 2015, 45(6): 933-941.]
- [62] 王栋. 阿拉善与华北地块晚古生代构造关系:来自沉积和物源方面的约束[D]. 西安:西北大学,2019:1-73. [Wang Dong. Late Paleozoic tectonic relationship between Alxa and North China Blocks: Constraints from sedimentology and provenance [D]. Xi'an: Northwest University, 2019: 1-73.]
- [63] 杨明慧,刘池洋,兰朝利,等. 鄂尔多斯盆地东北缘晚古生代陆表海含煤岩系层序地层研究[J]. 沉积学报,2008,26(6):1005-1013. [Yang Minghui, Liu Chiyang, Lan Chaoli, et al. Sequence stratigraphy of Late Paleozoic coal-bearing measures in northeastern Ordos Basin [J]. Acta Sedimentologica Sinica, 2008, 26(6): 1005-1013.]
- [64] 朱锐,张昌民,杜家元,等. 珠江口盆地新近纪海平面升降过程及其对砂体的控制[J]. 高校地质学报,2015,21(4):685-693. [Zhu Rui, Zhang Changmin, Du Jiayuan, et al. Controls of Neogene sea level change on sand bodies in the Pearl River Mouth Basin [J]. Geological Journal of China Universities, 2015, 21(4): 685-693.]

Genetic Mechanism and Depositional Processes of Sandy Sediments from the Carboniferous Yanghugou Formation Along the Western Margin of the Ordos Basin and Its Adjacent Areas

ZHU ShuYue¹, LIU Lei^{1,2}, WANG Feng^{1,2}, HOU YunDong³, WANG ZhiWei¹, ZHANG ChengGong^{1,2}, FU SiYi^{1,2}, CHEN HongDe^{1,2}, ZHANG JingQi¹

1. Institute of Sedimentary Geology, Chengdu University of Technology, Chengdu 610059, China

2. State Key Laboratory of Oil and Gas Reservoir Geology and Exploitation, Chengdu University of Technology, Chengdu 610059, China

3. Exploration and Development Research Institute of PetroChina Changqing Oilfield Company, Xi'an 710000, China

Abstract: The depositional period of the Yanghugou Formation in the western margin of the Ordos Basin was a resurrected aulacogen after the Caledonian movement. The Yanghugou Formation has a wide stratigraphic distribution area, large thickness variations, well-developed source-reservoir-caprock association, and huge exploration potential. Owing to the strong tectonic movements and frequent changes in the sedimentary environment, the sedimentary genesis of the sandy sediments are complicated. Currently, there is a lack of systematic research on the genetic mechanism of the Yanghugou Formation sandy sediments. A single depositional model cannot fully summarize the sedimen-

tary characteristics and distribution laws of various sandy sediments. In this study, six types of lithofacies associations were identified through field profile, core observation, drilling data, provenance analysis, and other research methods. Based on the lithology, grain size, sedimentary structure, and sandy sediment distribution characteristics in various periods, we conduct a systematic discussion on its genetic mechanism and dispersion process. The sandy sediments of the Yanghugou Formation in the western margin of the Ordos Basin are mainly by fluvial deltas, tide-controlled deltas, fan deltas, barrier island coasts, barrier-free coasts, and slump gravity flows. The overall climate of the Yanghugou Formation was humid, and the sea level gradually rose during the deposition of the 3rd the 2nd member of the Yanghugou Formation, and then gradually decreased after the 2nd member of the Yanghugou Formation reached the highest level. The sedimentary period of the 3rd member of the Yanghugou Formation was the early stage of rifting. Tide-controlled and fan delta sandy sediments were primarily developed in the northern region of the study area. Tidal sand ridges can be seen in the central part. The southern sandy sediments are generally barrier-free coastal sediments. The sedimentary period of the 2nd member of the Yanghugou Formation is the climax of rifting. The increase of landform drop leads to the rapid deepening of the water body, and the sandy sediments were primarily distributed on the edge of the basin. Point slump gravity flow sandy sediments developed in the deep-water of the center of the basin. The tidal sand ridges near the central paleo-uplift in the East is gradually transformed into barrier sand dams, and the high parts of the paleo-uplift were deposited with tidal flats and lagoons. During the sedimentary period of the 1st member of the Yanghugou Formation, the tectonic activity weakened and the Ordos Basin gradually connected to the east and west. The provenance supply was sufficient and the landform becomes slower, and a large area of fluvial delta sandy sediments with progradation characteristics are developed. The genetic mechanism of the Yanghugou Formation sandy sediments is affected by many factors, such as tectonic movement, paleogeomorphic evolution, provenance supply, paleoclimate, sedimentary dynamic environment, and so on. However, the distribution of sandy sediments and the process of sandy sediments dispersion are controlled by tectonic activities and paleogeographic evolution. The research results are of great significance for enriching the oil and gas exploration theory in the Ordos Basin and the genetic mechanism of rifted basin sandy sediments.

Key words: lithofacies association; genetic mechanism; control factors; sandy sediments distribution; Yanghugou Formation; western margin of Ordos Basin